Metabolites profiling of Sapota fruit pulp *via* a multiplex approach of gas and ultra performance liquid chromatography/mass spectroscopy in relation to its lipase inhibition effect

Mohamed A. Farag[1], Nermin Ahmed Ragab[2] and Maii Abdelnaby Ismail Maamoun[2]

[1] Department of Pharmacognosy, Cairo University, Cairo, Egypt
[2] Department of Pharmacognosy, National Research Center, Giza, Egypt

ABSTRACT

Background. Sapota, *Manilkara zapota* L., are tasty, juicy, and nutrient-rich fruits, and likewise used for several medicinal uses.

Methods. The current study represents an integrated metabolites profiling of sapota fruits pulp *via* GC/MS and UPLC/MS, alongside assessment of antioxidant capacity, pancreatic lipase (PL), and α-glucosidase enzymes inhibitory effects.

Results. GC/MS analysis of silylated primary polar metabolites led to the identification of 68 compounds belonging to sugars (74%), sugar acids (18.27%), and sugar alcohols (7%) mediating the fruit sweetness. Headspace SPME-GC/MS analysis led to the detection of 17 volatile compounds belonging to nitrogenous compounds (72%), ethers (7.8%), terpenes (7.6%), and aldehydes (5.8%). Non-polar metabolites profiling by HR-UPLC/MS/MS-based Global Natural Products Social (GNPS) molecular networking led to the assignment of 31 peaks, with several novel sphingolipids and fatty acyl amides reported for the first time. Total phenolic content was estimated at 6.79 ± 0.12 mg gallic acid equivalent/gram extract (GAE/g extract), but no flavonoids were detected. The antioxidant capacities of fruit were at 1.62 ± 0.2, 1.49 ± 0.11, and 3.58 ± 0.14 mg Trolox equivalent/gram extract (TE/g extract) *via* DPPH, ABTS, and FRAP assays, respectively. *In vitro* enzyme inhibition assays revealed a considerable pancreatic lipase inhibition effect (IC_{50} = 2.2 ± 0.25 mg/mL), whereas no inhibitory effect towards α-glucosidase enzyme was detected. This study provides better insight into sapota fruit's flavor, nutritional, and secondary metabolites composition mediating for its sensory and health attributes.

Subjects Biochemistry, Food Science and Technology, Plant Science

Keywords *Manilkara zapota* L., SPME-GC/MS, UPLC/MS, GNPS molecular networking, Lipase inhibitor, Antioxidant

Submitted 12 April 2024
Accepted 23 July 2024
Published 29 August 2024

Corresponding author
Mohamed A. Farag,
mohamed.farag@pharma.cu.edu.eg

Academic editor
Prof. Hamid Mukhtar

Additional Information and Declarations can be found on page 17

DOI **10.7717/peerj.17914**

INTRODUCTION

One of the biggest issues today is obesity, WHO predicts that by 2025, around 167 million individuals will encounter health problems owing to obesity (*WHO, 2022*). Obesity affects all of the body's organs leading to a wide range of metabolic disorders, such as diabetes

How to cite this article Farag MA, Ragab NA, Maamoun MAI. 2024. Metabolites profiling of Sapota fruit pulp *via* a multiplex approach of gas and ultra performance liquid chromatography/mass spectroscopy in relation to its lipase inhibition effect. *PeerJ* **12**:e17914
http://doi.org/10.7717/peerj.17914

and hyperlipidemia, especially in low and middle-income countries. Current therapeutic strategies to manage hyperglycemia and hyperlipidemia depend on the inhibition of digestive enzymes. Thereby, relying on pancreatic lipase inhibitors is a potential approach to reduce fat absorption and weight while inhibiting α-glucosidase enzyme can lead to the slower digestion of carbohydrates and postprandial glucose control (*Prieto-Rodríguez et al., 2022*). Dietary antioxidants could potentially contribute to the prevention and management of obesity. These phytoconstituents have a regulatory effect on cellular processes involved in adipose tissue function and energy metabolism (*Almoraie & Shatwan, 2024*).

Several approved anti-obesity drugs have now been discontinued due to their adverse effects such as bloating, flatulence, oily stools, diarrhea, abdominal pain, and reduction in fat-soluble vitamin absorption (*Oshiomame Unuofin, Aderonke Otunola & Jide Afolayan, 2018*). Additionally, various oral anti-diabetic drugs are contraindicated to other medications (*Chaudhury et al., 2017*). Thus, it is crucial to find an anti-obesity medication from natural resources, especially with various natural products reported to reduce body weight and blood glucose levels.

Sapotaceae is a family of tropical, evergreen trees and shrubs that comprises more than 50 genera and 1,100 species. One of the most famous genera in the Sapotaceae family is *Manilkara* with *ca*. 80 species. The trees of *Manilkara zapota* (L.) Van Royen is the most extensively grown species (*The Plant List, 2010*; *Madani et al., 2018*).

Manilkara zapota (L.) fruits, also known as sapota, sapodilla, and chicozapote, are uniquely delicious, with a delicate, grainy feel and pleasant smell. The fruit comprises a wide array of nutrients, minerals, and polyphenols with diverse biological activities (*Siddiqui et al., 2014*). Unripe fruits are astringent in taste due to high levels of catechins, chlorogenic acid, gallotannins, and proanthocyanidins (*Ma et al., 2003*). Aside from phenolics, fruits are also rich in triterpenoids represented by β-amyrin-3-(3′-dimethyl) butyrate and lupeol-3-acetate (*Fayek et al., 2013*). The fruit aqueous extract exhibits potential anti-hypercholesterolemic, antihyperglycemic, and antioxidant effects (*Fayek et al., 2013*). Previous results revealed a decrease in body weight and a good influence on biomarkers, *viz*, insulin, glycemia, cholesterol, and triglycerides in animals treated with *M. zapota* fruit juice, highly indicating the antidiabetic and anti-obesity potentials of its fruit (*Barbalho et al., 2015*).

Metabolite profiling assesses the nutritional value and bioactive constituents of botanical samples mediating for their health benefits. The current study presents a multiplex approach employing gas chromatography coupled with mass spectrometry (GC/MS), and high-resolution ultra-high performance liquid chromatography coupled with tandem mass spectrometry (HR-UPLC/MS/MS) for profiling *M. zapota* (L.) fruit pulp targeting its aroma, non-volatile polar and non-polar metabolites to account for fruit sensory, nutritional, and health attributes. The aroma profile was assessed using solid phase micro-extraction (SPME), whereas primary polar metabolites *viz*. sugars were analyzed using GC/MS post-silylation. For large molecular weight non-polar metabolites analysis, HR-UPLC/MS/MS was employed aided by Global Natural Products Social (GNPS) molecular networking to assist in metabolites identification. In addition, total phenolics and flavonoids were determined for standardization, alongside lipase and α-glucosidase

inhibition activities of fruit extract. The main goal of this study is the identification and development of natural curing agents for metabolic disorders.

MATERIALS AND METHODS

Plant material and extraction process

The fresh fruit pulp of sapota (*Manilkara zapota* L.) was collected from Haryana Agriculture University, Hisar, India in December 2022. The plant sample was identified by Dr. Rupesh Deshmuk, Central University of Haryana, India. Fruits were immediately lyophilized by Telstar Laboratory Freeze Dryers, peeled and the pulp was taken, treated with liquid nitrogen powdered using mortar and pestle, and stored in closed, air-tight bags at −20 °C until further analysis. The extraction process was carried out following the previously mentioned procedure (*El-Akad, El-Din & Farag, 2023*). Using a homogenizer (Ultra-Turrax, IKA, Staufen, Germany) at 11,000 rpm, 5 X 60 s with 1 min break intervals, about 150 g of the crushed sample was mixed with six mL methanol containing 10 μg/mL umbelliferone (Sigma-Aldrich, St. Louis, MO, USA, purity ≥ 98%) that used as an internal standard and for MS calibration. Further processing, the extract was centrifuged at 3,000× g for 30 min after being vortexed for 1 min, filtered through a 22 μm pore size filter, and directly used for HR-UPLC-MS/MS analysis. For GC/MS, 100 μl was aliquoted in a glass vial and left to evaporate till dryness under a nitrogen stream. For bioassay, fruit pulp was extracted using 100% MeOH (Sigma Aldrich, St. Louis, MO, USA) till exhaustion and evaporated using rotavap under vacuum to yield dried yellowish residue stored at −20 °C till further assays.

Chemicals and fibers

The stableflex fiber used for solid phase micro-extraction (SPME) was covered by divinylbenzene/carboxen/polydimethylsiloxane (DVB/CAR/PDMS, 50/30 μm) and was obtained from Supelco (Oakville, ON, Canada). Chemicals were acquired from Sigma Aldrich (St. Louis, MO, USA). Milli-Q water and solvents were used for HR-UPLC/MS/MS analysis; formic acid and acetonitrile were of LC-MS grade and obtained from J. T. Baker (The Netherlands).

ABTS [2,20′azino-bis (3-ethylbenzothiazoline-6-sulfonic acid) diammonium salt] ≥ 98% purity, DPPH (2,2-diphenyl-1-picrylhydrazyl), ferric chloride for FRAP (ferric reducing antioxidant power), Trolox (6-hydroxy-2,5,7,8-tetramethyl-chromane-2-carboxylic acid; ≥97% purity), porcine pancreatic lipase (PL) enzyme type II, intestinal α-glucosidase, Orlistat, Acarbose from Sigma Aldrich Chemie GmbH (St. Louis, MO, USA).

GC/MS analysis of silylated primary polar metabolites of *M. zapota* fruit pulp

Analysis of primary metabolites in fruit pulp followed the exact procedure (*El-Akad, El-Din & Farag, 2023*), in triplicates under the same conditions. The derivatization process was compiled as follows; the dried methanol extract of fruits was derivatized using a silylating agent; N-methyl-N-(trimethylsilyl)-trifluoroacetamide (MSTFA) (150 μL equally diluted with anhydrous pyridine), incubated in an oven for 45 min at 60 °C (Yamato Scientific

DGS400 Oven, QTE TECHNOLOGIES, Hanoi, Vietnam), just before GC/MS analysis. Silylated compounds were separated on a column 30 m × 0.25-mm id × 0.25-m film (Rtx-5MS Restek, Bellefonte, PA, USA), and were analyzed under conditions described in *Farag et al. (2022)*. Analysis was done in triplicate under the same conditions along with a blank sample to evaluate the variation in biological samples.

SPME-GC/MS analysis of volatiles in *M. zapota* fruit pulp

Preparation and analysis of the aroma profile in fruit pulp were performed following the same conditions reported in (*Farag et al., 2022*). A quadrupole mass spectrometer connected to an Agilent 5977B GC/MSD (Santa Clara, CA, USA) was used fitted with a DB-5 column (Supelco, Bellefonte, PA, USA) 30 m × 0.25 mm i.d. × 0.25 m film thickness. The scan range of the MS spectrometer was adjusted at *m/z* 40–500 and EI mode at 70 eV. Analysis was done in triplicate under the same conditions along with a blank sample to evaluate the variation in biological samples.

Identification of volatile and non-volatile silylated components using GC/MS

Deconvolution of the GC/MS spectrum was first applied using AMDIS software (http://www.amdis.net). Detection of compounds was achieved by matching the retention indices (RI) of the detected peaks with those of the n-alkanes series (C8-C30), along with matching their mass spectra with respected databases; NIST011 and WILEY libraries, and standards whenever available.

High-resolution ultra high-performance liquid chromatography coupled with tandem mass spectrometry (HR-UPLC/MS/MS) analysis of non-polar metabolites

HR-UPLC/MS/MS analysis was performed using an ACQUITY UPLC system (Waters, Milford, MA, USA) coupled with an HSS T3 (C_{18}) reversed-phase sorbent column (100 × 1.0 mm, particle size 1.8 μm; Waters). The analysis was accomplished following the precise guidelines as reported by *Hegazi et al. (2022)*. The tentative identification of compounds was based on the generated molecular formula at an error of 10 ppm or less, and by comparing MS^2 fragments with reported literature (*Böcker & Dührkop, 2016*).

Molecular networking and metabolites' annotation of HR-UPLC/MS/MS data

The HR-UPLC/MS/MS data (acquired in positive ion mode) from the fruit extract was used to create a molecular network (MN) using the GNPS website (http://gnps.ucsd.edu). The raw data underwent conversion to an open-source format (.mzML) using the MS Convert package (Proteowizard Software Foundation, Version 3.0.19330, USA). The transformed (.mzML) files were then uploaded to the GNPS platform using WinSCP (SFTP, FTP, WebDAV, and SCP client). GNPS parameters included fragment ion tolerance (0.5 u), minimum-matched fragments (four ions), minimum pairs cosine score (0.65), and parent mass tolerance (1.0 u), which were used to generate consensus spectra.

The spectral network was visualized with the aid of Cytoscape 3.9.1. Each spectrum was represented as a node in the visualization, with spectrum-to-spectrum connections forming

edges based on structural correspondence identified through MS analysis (*Xu et al., 2021*; *Zia-ur Rehman Gurgul et al., 2022*). For natural products dereplication, various databases were searched, including PubChem (https://pubchem.ncbi.nlm.nih.gov/), Metabolome database (https://hmdb.ca/), online lipid calculator database (http://www.mslipidomics.info/lipid-calc/), and LIPID MAPS (https://www.lipidmaps.org/).

For visualization of metabolite classes with sapota fruit, acquired tandem mass spectrometry data, and molecular networks were (MNS) constructed. In MNS, the mass spectrometric data were clustered according to the resemblances of their fragmented ions (*Ragheb et al., 2023*), and to aid in the identification of unknown peaks.

Total phenolic and total flavonoid contents assay

Fruit pulp extract was analyzed for total phenolic (TP) content and total flavonoid (TF) content, after being re-dissolved in 5% DMSO with 70% ethanol to yield a concentration of 1 mg/mL stock solution.

The evaluation of TP content was based on the Folin-Ciocalteu method, previously described by *Babotă et al. (2018)*. 20 μL sample were added to 100 μL Folin–Ciocalteu reagent at a ratio of 1:9 V/V and mixed well. 80 μL of Na_2CO_3 solution (1%) was added to the previous mixture. After 30 min of incubation at room temperature, the absorbance was measured at 760 nm. The result was represented as milligrams of gallic acid equivalent per gram sample (mg GAE/g extract), after triple measurements (mean ± SD).

For TF content, aluminum chloride assay was used (*Babotă et al., 2018*). A 100 μL sample was added to 100 μL of 2% aluminum trichloride/methanol. After 10 min incubation at room temperature, the absorbance was measured at 415 nm. Results were expressed as milligrams of rutin equivalent per gram sample (mg RE/g extract), after triple measurements (mean ± SD). In the two tests, the absorbances were analyzed in 96-well plates (SPECTROstar® Nano Multi-Detection Microplate Reader; BMG Labtech, Ortenberg, Germany).

In vitro antioxidant assays

Two assays depending on the free radical scavenging actions; DPPH (1,1-diphenyl-2-picrylhydrazyl) and ABTS (2,2′-azino-bis(3-ethylbenzothiazoline) 6-sulfonic acid), along with the ferric reducing antioxidant power (FRAP) technique for ferric reducing capacity, were applied following the protocols of *Babotă et al. (2018)*. Initially, the extract was dissolved in 70% ethanol to get a concentration of 1mg/mL. The absorbances were measured in 96-well plates (SPECTROstar® Nano Multi-Detection Microplate Reader; BMG Labtech, Ortenberg, Germany). A calibration curve was established using different concentrations of Trolox, a standard antioxidant substance. The resulting data were reported as mg of Trolox equivalents per gram sample (mg TE/g extract) in each case, after triple measurements (mean ± SD).

The DPPH free radical scavenging assay: 30 μL of the fruit methanol extract was mixed with 0.004% DPPH methanol solution and incubated for 30 min in the dark at room temperature. Absorbance was measured at 517 nm.

For ABTS free radical scavenging assay: $ABTS^+$ radical was prepared by adding 2.45 mM potassium persulfate to 7 mM ABTS solution, leaving the mixture to stand in the dark

and room temperature for 12 h. The resulting solution was further diluted with distilled water till absorbance reached 0.7 ± 0.02 at 734 nm and then mixed with fruit extract and incubated for 30 min at room temperature. The absorbance was measured at 734 nm.

For FRAP reducing capacity: FRAP reagent was prepared by blending acetate buffer (0.3 M, pH 3.6), 2,4,6-tris(2-pyridyl)-s-triazine (TPTZ) (10 mM) mixed with ferric chloride (20 mM) in 40 mM HCl at a ratio of 10:1:1(V/V/V). The reagent was added to the diluted fruit sample, mixed, and incubated for 30 min of at room temperature and absorbance was measured at 593 nm.

In vitro enzyme inhibition assays

The crude porcine PL type II enzyme was suspended in Tris-HCL buffer (2.5 mmol, adjusting pH at 7.4 with 2.5 mmol NaCl), mixing with a stirrer for 15 min, to get a concentration of 200 U/mL (5 mg/mL). The sample was incubated with 0.1 mL of PL solution for 5 min at 37 °C then *p*-nitrophenyl butyrate (*p* NPB) substrate (10 mM in acetonitrile) was added. Inhibition activity was measured colorimetrically based on *p*-nitrophenol release (at 410 nm compared to a blank of denatured enzyme), following a modified method mentioned by *Bustanji et al. (2011)*. The experiment was run in triplicate and percentage inhibition represented the average of three observations using two concentrations at 5 & 10 mg/mL of the extract, expressed in terms of IC_{50} (Half-maximal inhibitory concentration). Orlistat was used as a positive control as a standard PL inhibitor.

α-glucosidase inhibitory action was measured following the previously reported protocol (*Tanase et al., 2019*). In a 96-well plate, 50 µL of yeast α-glucosidase (1 U/mL) was mixed with equal volumes of diluted sample, 100 mM phosphate buffer (pH 6.8), and the substrate (5 mM *p*-nitrophenol- α-D-glucopyranoside (*p*-NPG). After an incubation period at 37 °C for 20 min, the color was formed due to *p*-nitrophenol release at 405 nm, and acarbose was used as a positive control. IC_{50} value was calculated from three measurements of the two tested extract doses at 5 & 10 mg/mL. In both tests, the results were calculated as the concentration that inhibited 50% of the enzyme according to the equation. Percentage of enzyme inhibition = (Ac -As / Ac) X 100, where Ac is the absorbance of the control and As is the absorbance of the sample.

RESULTS & DISCUSSION

Metabolites profiling of silylated primary polar metabolites in *M. zapota* fruit pulp as analyzed *via* GC/MS

GC/MS analysis of the non-volatile primary metabolites in fruit was carried out post-silylation to present a comprehensive overview of metabolites (Fig. 1), and to further account for nutritional and sensory attributes in fruits. As listed in Table 1, 68 compounds belonging to 11 chemical classes were detected. The most abundant metabolite classes included sugars, sugar acids, and sugar alcohols detected at 74.0, 18.27, and 7%, respectively. Other detected primary metabolites though at much lower levels included fatty acids/esters

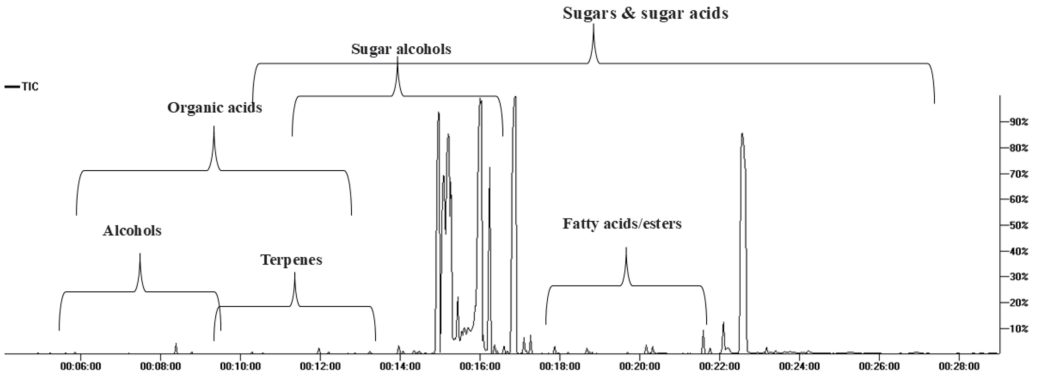

Figure 1 **Total ion chromatogram (TIC) of *M. zapota* fruit silylated polar metabolites analyzed using GC/MS.**

Full-size DOI: 10.7717/peerj.17914/fig-1

(0.22%), organic acids (0.22%), and inorganic acids (0.124%), along with traces of alcohols, terpenes, and nitrogenous compounds.

The high sugars' level in fruit imparts a sweet taste as typical in most fruits. As represented in the TIC (Fig. 1), sugars represented major primary metabolites detected in 22 peaks, especially mono-sugars to account for 75% of identified sugars. The most prominent forms included fructose (22.1%), D-glucose (16.6%), and mannose (16.5%). Sucrose (17.9%, peak 63) was the predominant disaccharide. Previous reports revealed that the total sugars in sapota fruit comprised *ca*. 46 to 52.2% of its weight (*Jadhav, Swami & Pujari, 2018*).

The high level of sugar acids represented by keto-D-gluconic acid (9.8%) and L-gluconic acid lactone (7.9%) imparts a slightly tangy and acidic taste, which might provide a balanced sensation alongside the intense sweet taste (*Karaffa & Kubicek, 2021*). Sugar alcohols with lower calorie intake than free sugars were represented by 5-deoxy-myo-inositol (6.7%). In addition to its low-calorie level, it reduces the body's resistance to insulin and aids in diabetes management (*Corrado & Santamaria, 2015*). Although organic acids were present at minor levels (0.22%), they were represented by 13 compounds, with oxalic and pyruvic acids as major forms.

Fatty acids/esters composition plays a role in nutrition and flavor in fruits, detected at 0.23% including glycerol monostearate, the monoglyceride ester with a sweet taste. Likewise, saturated fatty acid palmitic acid (0.045%) and its monoester, monopalmitin (0.054%), were detected suggesting that fruit is enriched with saturated fatty acids. To the best of our knowledge, this is the first detailed report on primary metabolites composition in sapota fruit.

Aroma profiling of *M. zapota* fruits pulp *via* SPME coupled to GC/MS

SPME-GC/MS analysis of aroma composition in *M. zapota* fruit revealed the detection of 17 compounds belonging to 8 chemical classes mostly dominated by nitrogenous compounds

Table 1 Identified silylated polar metabolites in *M. zapota* fruits using GC/MS, results expressed as a relative percentile % of the total peak area ($n = 3$). Results are represented as a relative percentile of the whole peak area ($n = 3$).

Peak	Rt. (min.)	KI	Metabolite	Average ± SD
			Alcohols	
1	4.81	1,042	2,3-Butanediol, 2TMS	tr.
2	4.93	1,049	2,3-Butanediol, 2TMS isomer	0.036 ± 0.002
3	5.127	1,061	1,3-Propanediol, 2TMS	tr.
10	7.201	1,190	1,2-Glycerol, 2TMS	0.014 ± 0.001
17	8.654	1,293	Butanetriol, 3TMS	0.009 ± 0.001
			Total	0.06 ± 0.005
			Fatty acids/esters	
52	17.14	2,030	Palmitic acid, TMS	0.045 ± 0.003
55	18.637	2,192	Linoleic acid, TMS	tr.
62	21.751	2,573	1-Monopalmitin, 2TMS	0.054 ± 0.020
64	23.164	2,765	Glycerol monostearate, 2TMS	0.121 ± 0.057
			Total	0.225 ± 0.081
			Organic acids	
4	5.238	1,068	Lactic Acid, 2TMS	0.027 ± 0.004
5	5.45	1,081	Glycolic acid, 2TMS	tr.
6	5.63	1,092	Pyruvic acid, 2TMS	0.048 ± 0.003
7	5.86	1,107	Oxalic acid, 2TMS	0.071 ± 0.020
8	6.26	1,131	Methylmalonic acid, TMS	tr.
9	6.693	1,159	Hydroxybutyric acid, 2TMS	0.006 ± 0.001
13	7.921	1,240.5	Benzoic acid, 3TMS	0.006 ± 0.001
18	8.785	1,302.5	Malonic acid, 3TMS	0.020 ± 0.005
19	8.859	1,308	Succinic acid, 2TMS	0.004 ± 0.002
22	10.185	1,403	Ketosuccinic acid, TMS	0.002 ± 0.000
24	11.24	1,488	Malic acid, 3TMS	tr.
26	12.207	1,566	Erythronic acid, 4TMS	0.025 ± 0.004
27	12.697	1,606	Tartaric acid, 4TMS	tr.
			Total	0.220 ± 0.040
			Inorganic acid	
15	8.39	1,274	Phosphoric acid, tri-TMS	0.124 ± 0.014
			Nitrogenous compounds/ Amino acid	
11	7.589	1,216.7	Uracil, TMS	0.002 ± 0.0
12	7.78	1,230	Urea, 2TMS	0.002 ± 0.0
14	8.102	1,253	L-Serine, 2TMS	0.001 ± 0.0
			Total	0.005 ± 0.001
			Terpenes	
16	8.517	1,283	Anethole	0.001 ± 0.001
21	9.3	1,339.4	α-Terpinyl acetate	0.002 ± 0.0
32	13.712	1,681	Curlone	0.002 ± 0.003
			Total	0.005 ± 0.005

(*continued on next page*)

Table 1 (*continued*)

Peak	Rt. (min.)	KI	Metabolite	Average ± SD
			Sugar acids	
20	9.18	1,331	Glyceric acid, 3TMS	0.005 ± 0.0
39	14.604	1,778	2-Keto-l-gluconic acid, 5TMS	0.008 ± 0.0
43	15.167	1,831.3	L-gluconic acid, 4TMS, lactone	7.934 ± 0.204
41	15.069	1,821.6	Mannonic acid, 5TMS, lactone	0.008 ± 0.007
45	15.182	1,833	Keto-gluconic acid, 5TMS	9.790 ± 1.663
51	17.087	2,024	D-Gluconic acid, 6TMS	0.101 ± 0.007
53	17.25	2,041.6	D-Glucuronic acid, 4TMS	0.292 ± 0.019
56	18.73	2,202	D-Galacturonic acid, 5TMS	0.041 ± 0.005
60	20.315	2,390	D-Glucuronic acid, 5-TMS	0.095 ± 0.021
			Total	18.274 ± 1.925
			Sugar alcohols	
25	11.96	1,546.5	Deoxyribitol, 4TMS	0.026 ± 0.003
34	13.963	1,720	Arabitol, 5TMS	0.128 ± 0.018
35	14.061	1,728.9	D-Glucitol, 6-deoxy, 5TMS	0.048 ± 0.004
36	14.343	1,754.3	D-Mannitol, 6TMS	0.010 ± 0.001
40	14.95	1,809.6	Myo-inositol, 5-deoxy, 5TMS	6.691 ± 0.292
54	17.859	2,108	Myo-Inositol, 6TMS	0.096 ± 0.011
			Total	7.000 ± 0.329
			Sugars	
23	10.227	1,407	L-Threose, 3TMS	0.043 ± 0.003
28	12.87	1,622	Arabinose, 4TMS	0.020 ± 0.002
29	13.234	1654.6	Arabinopyranose, 4TMS	0.049 ± 0.007
30	13.277	1,658	Galactopyranose, 5TMS	0.002 ± 0.0
31	13.449	1,674	Arabinofuranose, 4TMS	0.003 ± 0.0
33	13.774	1,695	L-Rhamnose, 4TMS	0.002 ± 0.0
37	14.473	1,766	1-Deoxyglucose, 4TMS	0.012 ± 0.002
38	14.52	1,770	Mannopyranose, 6-deoxy, 4TMS	0.007 ± 0.0
42	15.077	1,822.4	Fructofuranose, 5TMS isomer	0.003 ± 0.003
44	15.172	1,831.6	Fructofuranose, 5TMS	11.392 ± 0.212
46	15.245	1,839	Fructofuranose, 5TMS isomer	5.919 ± 0.248
47	15.429	1,857	D- Galactofuranose, 5TMS	0.207 ± 0.023
48	16.064	1,920	Mannose, 5TMS	16.530 ± 0.091
49	16.225	1,936	D-Fructose, 5TMS	4.791 ± 0.214
50	16.87	2,000.5	D-Glucose, 5TMS	16.652 ± 0.457
57	18.8	2,211	Cellobiose, 8TMS	0.006 ± 0.003
61	21.58	2,551	Turanose, 8TMS	0.254 ± 0.057
63	22.559	2,682	Sucrose, 8TMS	17.963 ± 1.072
65	23.393	2,797	3-α-Mannobiose, 8TMS	0.033 ± 0.001
66	24.207	2,908.7	Melibiose, 8TMS	0.057 ± 0.004
67	28.528	3,503	Maltose, 8TMS	0.006 ± 0.003
68	28.7	3,527	β-Gentiobiose, 8TMS	0.052 ± 0.046
			Total	74.002 ± 2.449

(*continued on next page*)

Table 1 (*continued*)

Peak	Rt. (min.)	KI	Metabolite	Average ± SD
			Glycerolipids	
58	19.685	2,315	Glycerol- α galactopyranoside, 6TMS	0.041 ± 0.004
59	20.155	2,371	Glycerol-galactopyranoside isomer, 6-TMS	0.044 ± 0.004
			Total	0.084 ± 0.008

Notes.
Tr, Traces

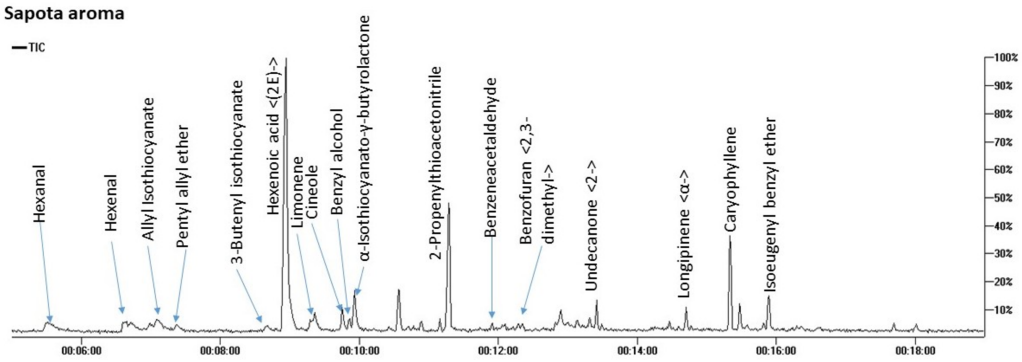

Figure 2 **Total ion chromatogram (TIC) of *M. zapota* fruit volatile constituents analyzed using SPME-GC/MS.**

Full-size DOI: 10.7717/peerj.17914/fig-2

amounting to 71.7%. Other classes included ethers (7.8%), terpenes (7.6%), and aldehydes (5.8%) as represented in Fig. 2 and Table 2.

The identified nitrogenous compounds (peaks 3, 5, 10, and 11) were detected for the first time in the fruit belonging to isothiocyanates, a hydrolysis product of glucosinolates. The major compound was 3-butenyl isothiocyanate (64.3%), alongside allyl isothiocyanate (2.8%). The presence of ethers in fruit provides specific fragrances, represented by benzyl isoeugenol ether (4.2%), peak 17, in addition to pentyl allyl ether (3.1%), peak 4, and cineole, peak 8 (*Kirsch & Buettner, 2013*).

As typical in fruit aroma, a considerable amount of mono- and sesquiterpenes were detected amounting (7.6%) of the total aroma composition, with β-caryophyllene (5.42%), peak 16, and limonene (1.54%) peak 7 as major components. β-Caryophyllene was previously detected in sapota fruit volatiles using steam distillation (*Pino, Marbot & Aguero, 2003*). Aldehydes, which accounted for 5.8% of the total fruit aroma, likely contribute to the fruit scent and likewise, protect against their deterioration due to potential antibacterial action (*Aljaafari et al., 2022*). The major form was hexanal at 4% to impart an apple-like odor (*Plotto, Bai & Baldwin, 2017*), alongside benzyl alcohol (2.6%) of a light fragrant smell (*Kulkarni & Mehendale, 2005*) and all to contribute to sapota fruit-specific scent.

Table 2 Volatile compounds in *M. zapota* fruits as analyzed by SPME coupled to GC/MS. Results are represented as a relative percentile of the whole peak area ($n = 3$).

Peak	Rt. (min.)	KI	Metabolite	Percent ±SD
			Aldehydes	
1	5.492	913	Hexanal	4.133 ± 0.96
2	6.603	1,096	3-Hexenal, (Z)-	1.208 ± 0.52
12	12.29	1,573	Benzene acetaldehyde	0.438 ± 0.15
			Total	5.78 ± 1.62
			Nitrogenous compounds	
3	7.083	1,176	Allyl Isothiocyanate	2.80 ± 0.22
5	8.94	1,313	3-Butenyl isothiocyanate	64.33 ± 1.96
10	10.56	1,433	α-Isothiocyanato-γ-butyrolactone	4.54 ± 0.35
11	11.29	1,492	2-Propenylthioacetonitrile	0.02 ± 0.01
			Total	71.69 ± 2.55
			Ethers	
4	7.136	1,186	Pentyl allyl ether	3.14 ± 0.29
8	9.86	1,379	Cineole <1,8->	0.46 ± 0.12
17	15.88	1,902	Isoeugenyl benzyl ether	4.23 ± 0.79
			Total	7.825 ± 1.20
			Acids	
6	9.35	1,343	Hexenoic acid <(2E)->	1.73 ± 0.51
			Terpenes	
7	9.75	1,371	Limonene	1.54 ± 0.27
15	14.699	1,786	Longipinene <α->	0.62 ± 0.09
16	15.33	1,847	Caryophyllene	5.42 ± 0.63
			Total	7.59 ± 0.99
			Alcohol	
9	9.93	1,384	Benzyl alcohol	2.59 ± 0.41
			Furan	
13	12.89	1,623	Benzofuran <2,3-dimethyl->	2.01 ± 0.56
			Ketone	
14	13.48	1,677	Undecanone <2->	0.79 ± 0.34

Non-polar metabolites profiling of *M. zapota* fruit as analyzed *via* HR-UPLC/MS/MS

Considering that GC/MS can only detect low molecular weight polar phytochemicals in food, and to provide a comprehensive composition of sapota fruit metabolome, HR-UPLC/MS/MS was employed to complement GC/MS and target large molecular weight lipids (*Islam et al., 2021*). Herein, a list of tentatively identified metabolites of *M. zapota* fruit is presented in Table 3, along with their chromatographic and spectroscopic data (Fig. 3). Major identified metabolites contained lipoidal components *e.g.*, fatty acyl amides, phospholipids, and sphingolipids, and contrary to low levels of lipids detected using GC/MS more suited for polar chemicals profiling. Other classes detected at minor levels included fatty acyl esters, nitrogenous compounds, glycol, amino acids, and diethanolamines. To aid in metabolites assignment, molecular networking was used for HR-UPLC/MS/MS

Table 3 Major non polar metabolites annotated in *M. zapota* fruit methanol extract via HRUPLC/MS/MS in positive ion mode.

Peak No.	Rt (min.)	Mol. Ion $(M+H)^+$	Error (ppm)	Molecular formula	MS/MS fragments	Identification	Class
1	0.987	166.0862	+0.33	$C_9H_{11}NO$	121, 120, 103	Phenylalanine	Amino acid
2	2.476	139.0755	−1.04	$C_8H_{10}O_2$	124, 121, 120	Styrene glycol	Alcohol
3	4.622	262.2371	+2.18	$C_{14}H_{31}NO_3$	226, 122	Tetradecaphytosphingosine	Sphingolipid
4	5.459	230.2474	+1.92	$C_{14}H_{31}NO$	213, 212, 109	Unknown	Nitrogenous
5	5.631	290.2688	+0.59	$C_{16}H_{35}NO_3$	272, 254,242	*LCBs (16;0)*	Sphingolipid
6	5.645	272.2576	+2.97	$C_{16}H_{33}NO_2$	254, 236, 224	Hexadecasphingosine	Sphingolipid
7	5.73	288.2527	+2.16	$C_{16}H_{33}NO_3$	227, 116, 102	Unknown amide	Nitrogenous lipid
8	5.964	316.2836	+3.24	$C_{18}H_{37}NO_3$	298,286, 281, 280, 262, 256, 141	Dehydrophytosphingosine	Sphingolipid
9	6.388	302.3047	+2.18	$C_{18}H_{39}NO_2$	284, 106, 102	Tetradecyldiethanolamine	Nitrogenous lipid
10	6.41	318.2997	+1.8	$C_{18}H_{39}NO_3$	300, 282, 264	Phytosphingosine	Sphingolipid
11	6.624	300.2891	+2.02	$C_{18}H_{37}NO_2$	282, 264	Sphingosine	Sphingolipid
12	7.063	415.2108	+2.48	$C_{20}H_{33}NO_6P$	354	Unknown PE	Phospholipid
13	7.145	330.3361	+1.69	$C_{20}H_{43}NO_2$	312,106,102	Hexadecyl diethanolamine	Nitrogenous lipid
14	7.289	478.2936	−1.64	$C_{23}H_{45}NO_7P$	337	LysoPE(0:0/18:2)	Phospholipid
15	7.833	454.2918	+2.24	$C_{21}H_{44}NO_7P$	313	LysoPE(0:0/16:0)	Phospholipid
16	8.014	358.368	−0.12	$C_{22}H_{47}NO_2$	340, 322, 270	Unknown	Unknown
17	10.59	256.2632	+1.14	$C_{16}H_{33}NO$	239, 238,209, 116, 102	Palmitamide	Fatty acyl amide
18	10.90	282.2785	+2.28	$C_{18}H_{35}NO$	247, 135, 121, 111, 102	Octadecenamide (Oleamide)	Fatty acyl amide
19	10.94	331.2843	−0.04	$C_{19}H_{38}O_4$	313, 109	Hexadecanoyl- glycerol	Fatty acyl ester
20	11.10	512.503	+1.41	$C_{32}H_{65}NO_3$	284	Tetradecanoyl-sphinganine	Sphingolipid
21	11.90	284.2937	+3.85	$C_{18}H_{37}NO$	200, 174,130, 116, 102	Octadecanamide (Steramide)	Fatty acyl amide
22	12.02	310.3099	+1.75	$C_{20}H_{39}NO$	293,292, 275, 268, 247, 135,121,111,109	Eicosenamide	Fatty acyl amide
23	12.25	359.3153	+0.8	$C_{21}H_{42}O_4$	341, 267, 239,112, 109	Glyceryl Monostearate	Fatty acyl ester
24	12.36	540.5345	+0.97	$C_{34}H_{69}NO_3$	307,286,285,284	Palmitoylsphinganine	Sphingolipid
25	12.40	568.566	+0.57	$C_{36}H_{73}NO_3$	285, 284, 264	Heneicosanoyl-pentadecasphinganine	Sphingolipid
26	13.08	312.3258	+0.94	$C_{20}H_{41}NO$	182, 116,112, 102	Icosanamide	Fatty acyl amide
27	13.15	338.3414	+1.01	C22H43NO	339, 321,320,303. 265,247, 135, 121	Erucamide	Fatty acyl amide
28	13.16	675.6761	+0.16	$C_{44}H_{86}N_2O_2$	338, 321, 303,121, 111,109	Erucamide dimer	Fatty acyl amide
29	13.27	732.5612	+1.13	$C_{40}H_{77}NO_{10}$	570, 552, 314, 262	Cerebroside(araliacerebroside)	Sphingolipid
30	14.14	302.305	+1.18	$C_{18}H_{39}NO_2$	285,284, 217	Octadecasphinganine	Sphingolipid
31	14.34	429.3715	+2.82	$C_{29}H_{48}O_2$	401, 371, 345, 205, 203, 187,165	Dehydrotocopherol	Tocopherol

Notes.
LCBs, long-chain bases sphingolipid

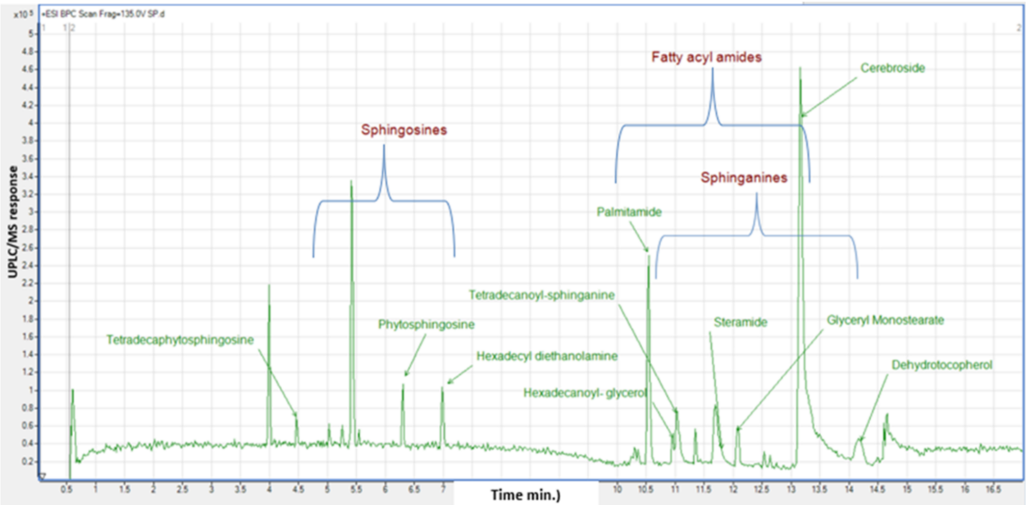

Figure 3 **Base peak chromatogram (BPC) of *M. zapota* fruit non polar metabolites analyzed using HR UPLC/MS/MS, in positive ion mode.**

Full-size DOI: 10.7717/peerj.17914/fig-3

dataset visualization. The MN afforded a total of 346 nodes, of which 141 clustered nodes and 205 self-looped nodes were detected (Fig. 4). The visual aid of MNS showed the diverse metabolite classes, which assisted in analog identification. The substantial clusters of positive MN belonged to oxylipids including cluster A (sphingosine and sphinganine), cluster B (fatty acyl amides), cluster C (phytosphingosine), and cluster D (fatty acyl esters), (Fig. 4).

Identification of fatty acyl amides

Fatty acyl amides, a subclass of lipids, exist as bioregulators for lipids in plants and are formed through amidation of fatty acids (*Tanvir, Javeed & Rehman, 2018*). Seven fatty acyl amides were identified in sapota fruit extract based on neutral losses of 14 amu, indicative of an acyl group (Fig. S1). Further, the annotation of saturated fatty acyl amides $[M + H]^+$ at *m/z* 256.263, 284.293, and 312.325 was based on their abundant fragments at *m/z* 102 ($C_5H_{10}NO$) and *m/z* 116 ($C_6H_{12}NO$). The presence of a single unsaturation in the alkyl chain of acyl amides alters product ion dramatically, as fragmentation differed with daughter ions corresponding to the combined neutral losses (−35 Da) of H_2O and NH_3 in the amide group. Distinct fragments at *m/z* 247 for the successive losses of water and ammonia moieties along with multiple losses of CH_2were recognized in MS^2 spectra of assigned unsaturated acyl amides. Conclusively, the whole loss of the acyl chain and formation of 9-carbon and 10-carbon macrocyclic dieneyl cation yielded daughter ions at *m/z* 135 and 121 and aided in structural elucidation of that subclass (*Murphy, 2014*).

Peaks 17, 18, 21, 22, 26, 27 and 28 exhibited molecular ions $[M+H]^+$ at *m/z* 256.26, 282.27, 284.29, 310.30, 312.325, 338.34 and 675.67 in MS/MS spectra with distinctive fragment ions of fatty acyl amides; palmitamide, octadecenamide (oleamide), octadecanamide (steramide), eicosenamide icosanamide, erucamide and erucamide dimer, respectively, cluster B in MN (Fig. 4). These metabolites are reported here for the first time

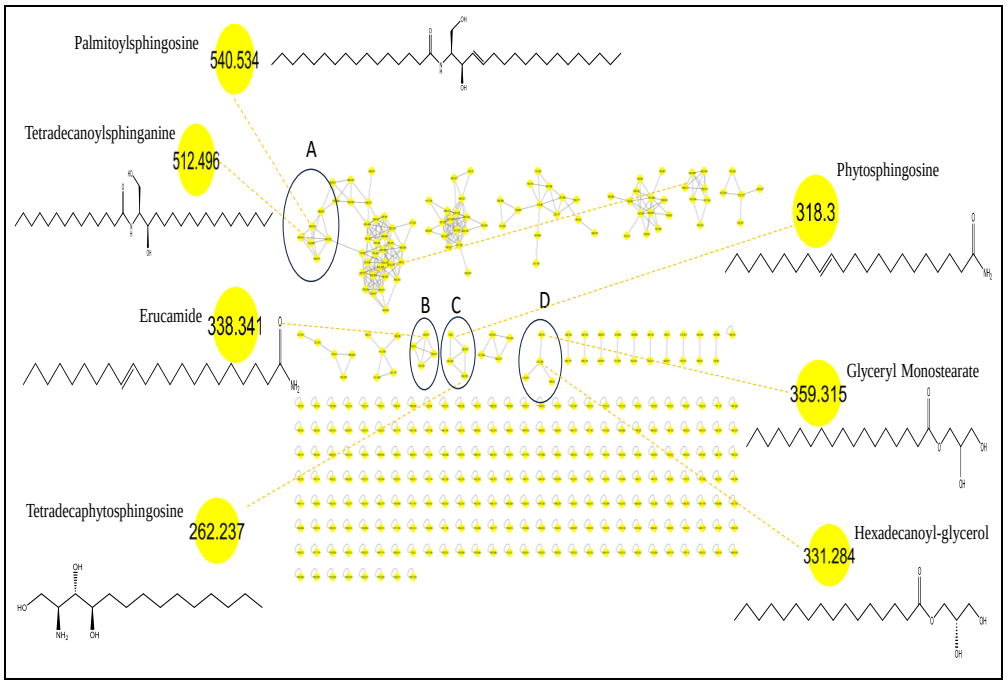

Figure 4 **Molecular networks created using MS/MS data from *M. zapota* fruit.**
Full-size DOI: 10.7717/peerj.17914/fig-4

in sapota fruit, and likely to account for a wide array of therapeutic indications such as treatment of bacterial infections, cancer, inflammations, and metabolic disorders (*Tanvir, Javeed & Rehman, 2018*). Steramide was detected previously in sapota leaves (*Tamsir et al., 2020*).

Identification of sphingolipids

The identified sphingolipids were detected in clusters A and C in the GNPS network (Fig. 4). Sphingosine is the major form present in this class and is assigned in peaks (3, 6, 8, 10, and 11), followed by the sphinganine class which was observed in BPC in peaks (20, 24, 25, and 30). The lipophilicity, formula composition, and fragmentation pattern suggest that these peaks are sphingolipid conjugates.

Most of the sphingolipids and their dihydro equivalents fragment to backbone ions with *m/z* 264 in positive ion mode as a key for the identification of sphingolipids (*Otify et al., 2019*). Most notably, product ion (*m/z* 284) is for sphinganine, whereas product ion at *m/z* 282 corresponds to sphingosine (Fig. S2).

For example, peak 8 exhibited a molecular formula [$C_{18}H_{37}NO_3$ (*m/z* 316.2836)], such a formula matches the class of sphingoid bases (that is non-phosphorylated plant sphingolipids) belonging to basic sphingoid compounds, either dehydrophytosphingosine, or 6-hydroxysphingosine (*Lénárt et al., 2021*). The fragmentation pattern showed product ions at *m/z* 280 and 262 corresponding to losses of 2 and 3 H_2O molecules, respectively, and assigning it as dehydrophytosphingosine.

Peak 3 showed fragmentation pattern of tetradecaphytosphingosine, based on the neutral loss of two water molecules and an alkyl chain ($C_{10}H_{20}$, 140 Da) at *m/z* 226 and 122 (Table 3). *Sphingolipid* long-chain base (LCB) was detected in peak 5 showing fragment ions at *m\z* 272, 254, 242 (*Qu et al., 2018*). The cerebroside (peak 29) with $(M+H)^+$ at *m\z* 732.56 ($C_{40}H_{77}NO_{10}$) and abundant ion at *m\z* 570 due to neutral loss of hexosyl and further loss of two water molecules to yield product ion at *m/z* 534 (*Kang et al., 1999*) and assigned as araliacerebroside (Fig. S3).

C16 sphinganine, a sphingolipid conjugate, was identified previously in *M. zapota* leaves (*Tamsir et al., 2020*), this study represents the first comprehensive profiling of sphingolipids in sapota fruits.

Identification of lysophosphatidylethanolamines

Lysophosphatidylethanolamines (Lyso-PE) were characterized in peaks 14 and 15 (Fig. S4) by the molecular formula of $C_xH_xNO_7P$ (*Ragheb et al., 2023*). LysoPE (0:0/18:2) and LysoPE (0:0/16:0) exhibited $(M+H)^+$ at *m/z* 478.29 and 454.29, respectively. The most abundant ions at *m/z* 337 and 313, in their positive-ion mass spectra, corresponded to the neutral loss of 141 Da of phosphoethanolamine (*Fang, Yu & Badger, 2003*), aiding in their assignment for the first time in sapota fruit.

Identification of ethanolamines

Peak 9 with $[M + H]^+$ at *m/z* 302 was assigned as tetradecyl diethanolamine ($C_{18}H_{39}NO_2$). The dehydration of the parent ion yielded *m/z* 284, with further cleavage of the carbon chain to yield fragment ion at *m/z* 102. The direct loss of carbon chain from quasi-molecular ion gave product ion at *m/z* 106 (Fig. S5), a key fragment of this class (*Zhang et al., 2022*). Peak 13 showed a similar fragmentation pattern assigned as N-hexadecyl diethanolamine $[M + H]^+$ at *m/z* 330.33 and fragment ions at *m/z* 312, 106 and 102. This is the first report on the presence of ethanolamines in sapota fruit. Ethanolamines are at the hub of various cellular processes, they stimulate the synthesis of phosphoethanolamine, a vital component to maintain human health. Moreover, ethanolamine prevents cardiovascular disease and ischemia (*Patel & Witt, 2017*).

Identification of fatty acyl esters

Fatty acyl esters were grouped in cluster D (Fig. 4) (peaks 23 & 19). This is the first report of the presence of fatty acyl esters in sapota fruit. Peak 23 showed the dehydration of precursor ion $[M + H]^+$ (*m/z* 359) that yielded fragment ion at *m/z* 341 (Fig. S6) attributed to an allylic cleavage and loss of glyceryl moiety yielding product ion at *m/z* 267 assigned as glyceryl monostearate. Similarly, peak 19 displayed a similar fragmentation scheme, suggesting the presence of hexadecanoyl glycerol with product ions at *m/z* 313 and 239.

Identification of tocopherols

MS^2 fragments of dehydrotocopherol (*m/z* 429.37) were detected in peak 31 and characterized by successive losses of alkyl groups to show fragmentation pattern; (*m/z* 401, 345, and 303), eventually the complete loss of side-chain together with the cleavage of chromene ring developed the product ion *m/z* 165 (Fig. S7).

Total phenolic and total flavonoid contents

The quantitative estimation of total phenolics and flavonoids in sapota fruit flesh extract revealed that it encompasses a moderate amount of phenolics (6.79 ± 0.12 mg GAE/g) and traces of flavonoids below our LOQ (limit of quantitation). The ripeness of the fruit results in a major change in its composition from an astringent taste owing to tannins and catechins, to a sweet taste due to the elevated sugar content. Fruit ripening had an impact on phenolic content due to the oxidation of phenolics by the action of polyphenol oxidase (PPO) enzyme (*Torres-Rodríguez et al., 2011*). As was previously reported, the higher phenolic and flavonoid contents were found in leaves, than peels, and the least was for the flesh, where values detected were at 14.15 ± 0.48, 1.23 ± 0.06, and 0.73 ± 0.1 μg GAE/100 g, respectively, for 70% ethanol extract of each organ (*Tamsir et al., 2020*).

In vitro antioxidant assays

Assessment of the antioxidant activity of sapota fruit pulp extract was carried out using DPPH, ABTS scavenging assays, and FRAP assay to estimate its reducing property. Results revealed moderate effects at 1.62 ± 0.2, 1.49 ± 0.11, and 3.58 ± 0.14 mg TE/g extract as per DPPH, ABTS, and FRAP assays, respectively. According to previous reports, the highest antioxidant activity was exhibited by leaf (92.96 ± 0.06%), then peel (91.98 ± 0.71%), much higher than that of fruit pulp (78.21 ± 0.04% of DPPH scavenging activity) as was reported in this study (*Tamsir et al., 2020*).

Metabolites profiling of fruit pulp showed that sphingoid bases and fatty acyl amides were the most abundant components, to likely contribute to the antioxidant activities. Prior studies proved that sphinganine inhibits the transport of cholesterol and low-density lipoprotein (*Tamsir et al., 2020*; *Roff et al., 1991*). Furthermore, previous findings confirm that monounsaturated fatty acids regulate several biochemical events (GABA, cannabinoid and anabolic pathways) within the cells (*Murphy, 2015*; *Divito & Cascio, 2013*). Additionally, other constituents may work together synergistically to boost antioxidant effectiveness (*Kumar et al., 2022*). Herein, several metabolites detected in the present study were reported for their antioxidant effect, including sugar alcohols, *viz*, mannitol (*Kang et al., 2007*), allyl isothiocyanates (*Caglayan et al., 2019*), palmitic acid, linoleic acid, (*Henry et al., 2002*), organic acids, *viz*, malic acid (*G¸asecka et al., 2018*), along with anethole (*Aprotosoaie et al., 2019*), curlone (*Jayaprakasha et al., 2002*), limonene (*El Omari et al., 2023*), cineole (*Hoch et al., 2023*).

In vitro enzymes inhibition assays

Fruit pulp extract was assessed for its hypolipidemic and antidiabetic activities *via in vitro* assays targeting the inhibition of pancreatic lipase (PL) and α-glucosidase enzymes, respectively. PL inhibitory assay tested the extract's influence on enzymatic activity and its potential for obesity management and lipid metabolic disorders. Results revealed that sapota fruit extract inhibited lipase enzyme by IC_{50} = 4.42 ± 0.5 mg/mL and 2.21 ± 0.25 mg/mL at sample concentrations of 10 and 5 mg/mL, respectively, compared to the standard drug, Orlistat which showed IC_{50} values of 0.16 and 0.08 mg/mL, Table 4.

Lipase enzyme plays a major role in fat metabolism. its downregulation leads to a decrease in low-density lipoprotein (LDL) and an increase in high-density lipoprotein

Table 4 Enzymes inhibitory actions of sapota fruit extract, at 2 concentrations, compared to the positive controls.

IC_{50} (mg/mL)	Pancreatic Lipase (PL) Inhibition Assay		α-Glucosidase inhibitory Assay	
Sample Conc.	SF ext.	Orlistat	SF ext.	Acarbose
10 mg/mL	4.42 ± 0.5	0.16	NA	0.5
5 mg/mL	2.21 ± 0.25	0.08	NA	0.16

(HDL) (*Liu et al., 2020*), and provides health benefits for obesity prevention, management, and its related disorders (*Marzouk et al., 2024*). In the current study, the major metabolites detected in sapota fruit included sphingolipids, fatty acyl amides, and phospholipids, which could relate to its potential lipase inhibitory effect.

Previous studies reported the efficacy of dietary sphingolipids as a highly effective nutritional aid in improving metabolic syndromes and their outcoming disease, including, atherosclerosis, obesity, type 2 diabetes mellitus, and non-alcoholic fatty liver disease (*Wang et al., 2021*). Additionally, supplementation of phytosphingolipids was found to lower plasma triglycerides, low-density lipoprotein cholesterol levels, and improve clearance of glucose (*Snel et al., 2010*). *Liu et al. (2015)* reported that dietary sphingolipids effectively lowered epididymal adipose tissue weights, inhibited hepatic triglycerides levels, and serum glucose, and suppressed lipid uptake, moreover, increased the rate of triglycerides catabolism.

Fatty acyl amide is involved in the metabolic homeostasis of the human system (*Tanvir, Javeed & Rehman, 2018*). Likewise, phospholipids, amphiphilic lipids rich in sapota pulp, have been implicated in exhibiting a favored impact on blood lipids by reducing TG, total cholesterol, and LDL levels (*Küllenberg et al., 2012*). Moreover, terpenoids detected by GC/MS are reported as pancreatic lipase inhibitors (*Singh et al., 2015*). Compared to the potential lipase inhibition effect in fruit pulp. There is no effect observed regarding the α-glucosidase inhibitory action. It was found that fruits were inactive against the enzyme compared to the positive drug control acarbose. This finding could be attributed to the decline in phenolic constituents and increased free sugars upon fruit maturation.

CONCLUSION

This study reports on the metabolic profile of sapota fruit pulp *via* UPLC/MS and GC/MS techniques. SPME-GC/MS analysis revealed 17 aroma compounds to account for fruit aroma. Concerning nutrient composition, GC/MS analysis revealed 68 peaks belonging primarily to sugars accounting for fruit sweetness, and high-calorie content. Thirty-one metabolites were annotated using HR-UPLC/MS/MS which are reported for the first time in sapota fruit. For standardization of fruit pulp in terms of its total phenolics and flavonoids, a moderate level of phenolics was detected, while no flavonoids were noted. The antioxidant assays revealed a moderate free radical scavenging effect *via* DPPH and ABTS assays, *versus* moderate reducing capacity by FRAP assay. Fruit pulp extract exerted a considerable pancreatic lipase inhibitory (PL) action *versus* no *a*-glucosidase inhibition effect likely attributed to moderate levels of phenolics and absence of flavonoids. The

current study presents a comprehensive profiling of phytochemicals to provide better insight into sapota fruit's nutritive and health benefits. Future research is recommended to identify the best extraction solvents targeting the recovery and yield of its phytochemicals. Also, the promising lipase inhibitory action of fruit pulp motivates investigating various extracts to determine the most effective one for identifying natural antiobesity agents of natural origin.

ACKNOWLEDGEMENTS

The authors are very grateful to Dr. Rupesh K. Deshmukh. Central University of Haryana, India for his kind help in the collection and authentication of sapota fruits.

ADDITIONAL INFORMATION AND DECLARATIONS

Funding

The authors received no funding for this work.

Competing Interests

Mohamed A Farag is an Academic Editor for PeerJ.

Author Contributions

- Mohamed A. Farag conceived and designed the experiments, performed the experiments, analyzed the data, prepared figures and/or tables, authored or reviewed drafts of the article, and approved the final draft.
- Nermin Ahmed Ragab performed the experiments, analyzed the data, prepared figures and/or tables, and approved the final draft.
- Maii Abdelnaby Ismail Maamoun performed the experiments, analyzed the data, prepared figures and/or tables, and approved the final draft.

Data Availability

The following information was supplied regarding data availability:

Raw data are available in the Supplemental Files.

Supplemental Information

Supplemental information for this article can be found online at http://dx.doi.org/10.7717/peerj.17914#supplemental-information.

REFERENCES

Aljaafari MN, Alkhoori MA, Hag-Ali M, Cheng W-H, Lim S-H-E, Loh J-Y, Lai K-S. 2022. Contribution of aldehydes and their derivatives to antimicrobial and immunomodulatory activities. *Molecules* **27(11)**:3589 DOI 10.3390/molecules27113589.

Almoraie NM, Shatwan IM. 2024. The potential effects of dietary antioxidants in obesity: a comprehensive review of the literature. *Healthcare (Switzerland, Basel)* **6;12(4)**:416. Multidisciplinary Digital Publishing Institute (MDPI) DOI 10.3390/healthcare12040416.

Aprotosoaie AC, Luca VS, Trifan A, Miron A. 2019. Antigenotoxic potential of some dietary non-phenolic phytochemicals. In: ur Rahman Atta, ed. *Studies in natural products chemistry*. vol. 60. Amsterdam, The Netherlands: Elsevier, 223–297.

Babotă M, Mocan A, Vlase L, Crişan O, Ielciu I, Gheldiu A-M, Vodnar D, Crişan G, Păltinean R. 2018. Phytochemical analysis, antioxidant and antimicrobial activities of *Helichrysum arenarium* (L.) Moench. and *Antennaria dioica* (L.) Gaertn. flowers. *Molecules* **23(2)**:409 DOI 10.3390/molecules23020409.

Barbalho SM, Bueno PCDS, Delazari DS, Guiguer EL, Coqueiro DP, Araújo AC, De Souza MDSS, Farinazzi-Machado FMV, Mendes CG, Groppo M. 2015. Antidiabetic and antilipidemic effects of *manilkara zapota*. *Journal of Medicinal Food* **18(3)**:385–391 DOI 10.1089/jmf.2013.0170.

Böcker S, Dührkop K. 2016. Fragmentation trees reloaded. *Journal of Cheminformatics* **8(1)**:5 DOI 10.1186/s13321-016-0116-8.

Bustanji Y, Al-Masri IM, Mohammad M, Hudaib M, Tawaha K, Tarazi H, Al Khatib HS. 2011. Pancreatic lipase inhibition activity of trilactone terpenes of *Ginkgo biloba*. *Journal of Enzyme Inhibition and Medicinal Chemistry* **26(4)**:453–459 DOI 10.3109/14756366.2010.525509.

Caglayan B, Kilic E, Dalay A, Altunay S, Tuzcu M, Erten F, Orhan C, Gunal MY, Yulug B, Juturu V, Sahin K. 2019. Allyl isothiocyanate attenuates oxidative stress and inflammation by modulating Nrf2/HO-1 and NF-κB pathways in traumatic brain injury in mice. *Molecular Biology Reports* **46(1)**:241–250 DOI 10.1007/s11033-018-4465-4.

Chaudhury A, Duvoor C, Reddy Dendi VS, Kraleti S, Chada A, Ravilla R, Marco A, Shekhawat NS, Montales MT, Kuriakose K, Sasapu A, Beebe A, Patil N, Musham CK, Lohani GP, Mirza W. 2017. Clinical review of antidiabetic drugs: implications for type 2 diabetes mellitus management. *Frontiers in Endocrinology* **24(8)**:6 DOI 10.3389/fendo.2017.00006.

Corrado F, Santamaria A. 2015. Myoinositol supplementation on insulin resistance in gestational diabetes. In: *Glucose intake and utilization in pre-diabetes and diabetes*. Academic Press, 229–234 DOI 10.1016/B978-0-12-800093-9.00019-3.

Divito EB, Cascio M. 2013. Metabolism, physiology, and analyses of primary fatty acid amides. *Chemical Reviews* **113(10)**:7343–7353. American Chemical Society DOI 10.1021/cr300363b.

El-Akad RH, El-Din MGS, Farag MA. 2023. How does *Lagenaria siceraria* (Bottle Gourd) metabolome compare to *cucumis sativus* (cucumber) F. Cucurbitaceae? A multiplex approach of HR-UPLC/MS/MS and GC/MS using molecular networking and chemometrics. *Foods* **12(4)**:771 DOI 10.3390/foods12040771.

El Omari N, Mrabti HN, Benali T, Ullah R, Alotaibi A, Abdullah ADI, Goh KW, Bouyahya A. 2023. Expediting multiple biological properties of limonene and α-pinene: main bioactive compounds of *pistacia lentiscus* l. essential oils. *Frontiers in Bioscience - Landmark* **28(9)**:229 DOI 10.31083/j.fbl2809229.

Fang N, Yu S, Badger TM. 2003. LC-MS/MS analysis of lysophospholipids associated with soy protein isolate. *Journal of Agricultural and Food Chemistry* **51(23)**:6676–6682 DOI 10.1021/jf034793v.

Farag MA, Ramadan NS, Shorbagi M, Farag N, Gad HA. 2022. Profiling of primary metabolites and volatiles in apricot (*prunus armeniaca* l.) seed kernels and fruits in the context of its different cultivars and soil type as analyzed using chemometric tools. *Foods* **11(9)**:1339 DOI 10.3390/foods11091339.

Fayek N, Monem AA, Mossa M, Meselhy M. 2013. New triterpenoid acyl derivatives and biological study of *Manilkara zapota* (L.) Van Royen fruits. *Pharmacognosy Research* **5(2)**:55–59 DOI 10.4103/0974-8490.110505.

Gąsecka M, Magdziak Z, Siwulski M, Mleczek M. 2018. Profile of phenolic and organic acids, antioxidant properties and ergosterol content in cultivated and wild growing species of Agaricus. *European Food Research and Technology* **244(2)**:259–268 DOI 10.1007/s00217-017-2952-9.

Hegazi NM, Khattab AR, Frolov A, Wessjohann LA, Farag MA. 2022. Authentication of saffron spice accessions from its common substitutes via a multiplex approach of UV/VIS fingerprints and UPLC/MS using molecular networking and chemometrics. *Food Chemistry* **367**:130739 DOI 10.1016/j.foodchem.2021.130739.

Henry GE, Momin RA, Nair MG, Dewitt DL. 2002. Antioxidant and cyclooxygenase activities of fatty acids found in food. *Journal of Agricultural and Food Chemistry* **50(8)**:2231–2234 DOI 10.1021/jf0114381.

Hoch CC, Petry J, Griesbaum L, Weiser T, Werner K, Ploch M, Verschoor A, Multhoff G, Bashiri Dezfouli A, Wollenberg B. 2023. 1 8-cineole (eucalyptol): a versatile phytochemical with therapeutic applications across multiple diseases. *Biomedicine and Pharmacotherapy* **167**:115467 DOI 10.1016/j.biopha.2023.115467.

Islam S, Alam MB, Ann HJ, Park JH, Lee SH, Kim S. 2021. Metabolite profiling of *manilkara zapota* l. Leaves by high-resolution mass spectrometry coupled with esi and apci and *in vitro* antioxidant activity, α-glucosidase, and elastase inhibition assays. *International Journal of Molecular Sciences* **22(1)**:1–17 DOI 10.3390/ijms22010132.

Jadhav SS, Swami SB, Pujari KH. 2018. Study the physico-chemical properties of sapota (*Achras Sapota* L.). *Trends in Technical & Scientific Research* **03(1)**:23–29 DOI 10.19080/TTSR.2018.03.555605.

Jayaprakasha GK, Jena BS, Negi PS, Sakariah KK. 2002. Evaluation of antioxidant activities and antimutagenicity of turmeric oil: a byproduct from curcumin production. *Zeitschrift Fur Naturforschung - Section C Journal of Biosciences* **57(9–10)**:828–835 DOI 10.1515/znc-2002-9-1013.

Kang K-W, Kwak S-H, Yun S-Y, Kim S-K. 2007. Evaluation of antioxidant activity of sugar alcohols using TOSC (total oxy-radical scavenging capacity) assay. *Toxicological Research* **23(2)**:143–150 DOI 10.5487/tr.2007.23.2.143.

Kang SS, Kim JS, Xu YN, Kim YH. 1999. Isolation of a new cerebroside from the root bark of *Aralia elata*. *Journal of Natural Products* **62(7)**:1059–1060 DOI 10.1021/np990018r.

Karaffa L, Kubicek CP. 2021. Production of organic acids by fungi. In: Zaragoza Ó, Casadevall A, eds. *Encyclopedia of mycology*. Elsevier, 406–419 DOI 10.1016/B978-0-12-809633-8.21066-2.

Kirsch F, Buettner A. 2013. Odor qualities and thresholds of physiological metabolites of 1 8-cineole as an example for structure activity relationships considering chirality aspects. *Chemistry & Biodiversity* **10(9)**:1683–1695 DOI 10.1002/cbdv.201300097.

Kulkarni SG, Mehendale HM. 2005. Benzyl alcohol. In: *Philip Wexler, encyclopedia of toxicology (second edition)*. Academic Press, 262–264 DOI 10.1016/B0-12-369400-0/00121-6.

Küllenberg D, Taylor LA, Schneider M, Massing U. 2012. Health effects of dietary phospholipids. *Lipids in Health and Disease* **11(1)**:3 DOI 10.1186/1476-511X-11-3.

Kumar V, Singh DD, Lakhawat SS, Yasmeen N, Pandey A, Singla RK. 2022. Biogenic phytochemicals modulating obesity: from molecular mechanism to preventive and therapeutic approaches. In: *Evidence-based complementary and alternative medicine. 2022(1)*. Hindawi Limited, 6852276 DOI 10.1155/2022/6852276.

Lénárt J, Gere A, Causon T, Hann S, Dernovics M, Németh O, Hegedűs A, Halász J. 2021. LC–MS based metabolic fingerprinting of apricot pistils after self-compatible and self-incompatible pollinations. *Plant Molecular Biology* **105(4–5)**:435–447 DOI 10.1007/s11103-020-01098-5.

Liu TT, Liu XT, Chen QX, Shi Y. 2020. Lipase inhibitors for obesity: a review. *Biomedicine and Pharmacotherapy* **1(128)**:110314 DOI 10.1016/j.biopha.2020.110314.

Liu X, Xu J, Xue Y, Gao Z, Li Z, Leng K, Wang J, Xue C, Wang Y. 2015. Sea cucumber cerebrosides and long-chain bases from *Acaudina molpadioides* protect against high fat diet-induced metabolic disorders in mice. *Food & Function* **6(11)**:3428–3436 DOI 10.1039/C5FO00602C.

Ma J, Luo XD, Protiva P, Yang H, Ma C, Basile MJ, Weinstein IB, Kennelly EJ. 2003. Bioactive novel polyphenols from the fruit of *Manilkara zapota* (Sapodilla). *Journal of Natural Products* **66(7)**:983–986 DOI 10.1021/np020576x.

Madani B, Mirshekari A, Yahia E, Golding JB. 2018. Sapota (*Manilkara achras* Forb.): factors influencing fresh and processed fruit quality. In: *Horticultural reviews, vol. 7, no. 45*. 2nd edition. New Jeysey: John Wiley and Sons Inc., 105–142 DOI 10.1002/9781119431077.ch4.

Marzouk MM, Ragheb AY, Youssef EM, Ragab NA, El-Taher EM, Garf IAE, Kassem MES. 2024. Isoflavone-rich extract of *trifolium resupinatum*: anti-obesity attributes with in silico investigation of its constituents. *Revista Brasileira de Farmacognosia* **34**:522–535 DOI 10.1007/s43450-023-00501-8.

Murphy RC (ed.) 2014. Tandem mass spectrometry of lipids: molecular analysis of complex lipids. London: Royal Society of Chemistry DOI 10.1039/9781782626350.

Murphy RC. 2015. Fatty acyl esters and amides. *New Developments in Mass Spectrometry* **2015(4)**:75–104 DOI 10.1039/9781782626350-00075.

Oshiomame Unuofin J, Aderonke Otunola G, Jide Afolayan A. 2018. *In vitro* a-amylase, a-glucosidase, lipase inhibitory and cytotoxic activities of tuber extracts of *Kedrostis africana* (L.) Cogn. *Heliyon* **4**:810.

Otify AM, El-Sayed AM, Michel CG, Farag MA. 2019. Metabolites profiling of date palm (*Phoenix dactylifera* L.) commercial by-products (pits and pollen) in relation to its antioxidant effect: a multiplex approach of MS and NMR metabolomics. *Metabolomics* **15(9)**:1–17 DOI 10.1007/s11306-019-1581-7.

Patel D, Witt SN. 2017. Ethanolamine and phosphatidylethanolamine: partners in health and disease. *Oxidative Medicine and Cellular Longevity* **2017(1)**:4829180 DOI 10.1155/2017/4829180.

Pino JA, Marbot R, Aguero J. 2003. Volatile components of sapodilla fruit (*Manilkara achras* L.). *Journal of Essential Oil Research* **15(6)**:374–375 DOI 10.1080/10412905.2003.9698614.

Plotto A, Bai J, Baldwin E. 2017. Fruits. In: *Springer handbook of odor*. Cham: Springer International Publishing, 27–28 DOI 10.1007/978-3-319-26932-0_9.

Prieto-Rodríguez JA, Lévuok-Mena KP, Cardozo-Muñoz JC, Parra-Amin JE, Lopez-Vallejo F, Cuca-Suárez LE, Patiño Ladino OJ. 2022. *In vitro* and *in silico* study of the α-glucosidase and lipase inhibitory activities of chemical constituents from *piper cumanense* (piperaceae) and synthetic analogs. *Plants* **11(17)** DOI 10.3390/plants11172188.

Qu F, Zhang H, Zhang M, Hu P. 2018. Sphingolipidomic profiling of rat serum by UPLC-Q-TOF-MS: application to rheumatoid arthritis study. *Molecules* **23(6)**:1–14 DOI 10.3390/molecules23061324.

Ragheb AY, Masoud MA, El Shabrawy MO, Farid MM, Hegazi NM, Mohammed RS, Marzouk MM, Aboutabl ME. 2023. MS/MS-based molecular networking for mapping the chemical diversity of the pulp and peel extracts from *Citrus japonica* Thunb.; in vivo evaluation of their anti-inflammatory and anti-ulcer potential. *Scientific African* **20**:e01672 DOI 10.1016/j.sciaf.2023.e01672.

Roff CF, Goldin E, Comly ME, Cooney A, Brown A, Vanier MT, Miller SP, Brady RO, Pentchev PG. 1991. Type C Niemann-pick disease: use of hydrophobic amines to study defective cholesterol transport. *Developemental Neuroscience* **13**:315–319.

Siddiqui MW, Longkumer M, Ahmad Md S, Barman K, Thakur PK, Kabir J. 2014. Postharvest biology and technology of sapota: a concise review. *Acta Physiologiae Plantarum* **36(12)**:3115–3122 DOI 10.1007/s11738-014-1696-4.

Singh G, Suresh S, Bayineni VK, Kadeppagari R-K. 2015. Lipase inhibitors from plants and their medical applications. *International Journal of Pharmacy and Pharmaceutical Sciences* **7**:1–5.

Snel M, Sleddering MA, Pijl H, Nieuwenhuizen WF, Frölich M, Havekes LM, Romijn JA, Jazet IM. 2010. The effect of dietary phytosphingosine on cholesterol levels and insulin sensitivity in subjects with the metabolic syndrome. *European Journal of Clinical Nutrition* **64(4)**:419–423 DOI 10.1038/ejcn.2009.154.

Tamsir MN, Esa MN, Nursalwah S, Omar C, Shafie NH. 2020. *Manilkara zapota* (L.) P. Royen: potential source of natural antioxidants. *Malaysian Journal of Medicine and Health Sciences* **2;16(6)**.

Tanase M, Cocsarcua G, Nicolescu G, Vodnar M, Crișan . 2019. Biological and chemical insights of beech (*fagus sylvatica* l.) bark: a source of bioactive compounds with functional properties. *Antioxidants* **8(9)**:417 DOI 10.3390/antiox8090417.

Tanvir R, Javeed A, Rehman Y. 2018. Fatty acids and their amide derivatives from endophytes: new therapeutic possibilities from a hidden source. *FEMS Microbiology Letters* **365(12)**:1–7 DOI 10.1093/femsle/fny114.

The Plant List. 2010. The Plant List. Version 1. *Available at http://www.theplantlist.org/*.

Torres-Rodríguez A, Salinas-Moreno Y, Valle-Guadarrama S, Alia-Tejacal I. 2011. Soluble phenols and antioxidant activity in mamey sapote (*Pouteria sapota*) fruits in postharvest. *Food Research International* **44(7)**:1956–1961 DOI 10.1016/j.foodres.2011.04.045.

Wang X, Wang Y, Xu J, Xue C. 2021. Sphingolipids in food and their critical roles in human health. *Critical Reviews in Food Science and Nutrition* **61(3)**:462–491 DOI 10.1080/10408398.2020.1736510.

WHO. 2022. World Obesity Day 2022 –accelerating action to stop obesity. *Available at https://www.who.int/news/item/04-03-2022-world-obesity-day-2022-accelerating-action-to-stop-obesity*.

Xu R, Lee J, Chen L, Zhu J. 2021. Enhanced detection and annotation of small molecules in metabolomics using molecular-network-oriented parameter optimization. *Molecular Omics* **17(5)**:665–676 DOI 10.1039/D1MO00005E.

Zia-ur Rehman Gurgul A, Youn I, Maldonado A, Wahid F, Che C-T, Khan T. 2022. UHPLC-MS/MS-GNPS based phytochemical investigation of *Equisetum arvense* L. and evaluation of cytotoxicity against human melanoma and ovarian cancer cells. *Saudi Journal of Biological Sciences* **29(6)**:103271 DOI 10.1016/j.sjbs.2022.03.021.

Zhang F, Li B, Wen Y, Liu Y, Liu R, Liu J, Liu S, Jiang Y. 2022. An integrated strategy for the comprehensive profiling of the chemical constituents of *Aspongopus chinensis* using UPLC-QTOF-MS combined with molecular networking Fengyu. *Pharmaceutical Biology* **60(1)**:1349–1364 DOI 10.1080/13880209.2022.2096078.